Beyond the Dipole Approximation: Angular-Distribution Effects in N_2 $1s$ Photoemission

O. Hemmers[1], P. Glans[1], H. Wang[1], R. Wehlitz[2], J.C. Levin[2], I.A. Sellin[2], R.C.C. Perera[3] and D.W. Lindle[1]

[1]Department of Chemistry, University of Nevada, Las Vegas, NV 89154-4003

[2]Department of Physics, University of Tennessee, Knoxville, TN 37996

[3]Lawrence Berkeley National Laboratory, Berkeley, CA 94720

INTRODUCTION

The electric-dipole ($E1$) approximation [1], applied to photoionization, leads to the well-known expression for the differential cross section [2],

$$\frac{d\sigma}{d\Omega} = \frac{\sigma}{4\pi}\left[1+\frac{\beta}{2}\left(3\cos^2\theta-1\right)\right], \tag{1}$$

which describes the angular distribution of photoelectrons from a randomly oriented sample created by 100% linearly polarized light. Here, σ is the partial photoionization cross section, and θ is the angle between the vector of the outgoing electron and the vector of linear polarization. The parameter β completely describes the angular distribution of photoelectrons, within the dipole approximation. In this approximation, all higher-order interactions, such as electric-quadrupole ($E2$) and magnetic-dipole ($M1$), are neglected. This assumption is justified by the argument that the strengths of the $E2$ and $M1$ interactions relative to electric-dipole effects are approximately equal to the ratio of the photoelectron's velocity to the speed of light [3], a ratio which is small except at very high energies.

Over the past two decades, the dipole approximation has facilitated a basic understanding of the photoionization process in atoms and molecules [2], as well as the application of photoelectron spectroscopy to a wide variety of condensed-phase systems.

The first hint of deviations from the dipole approximation was provided by Krause [4] in measurements using unpolarized x-rays [5]. A small deviation from the expected dipolar angular distribution at photon energies between 1 and 2 keV was observed and attributed to the influence of $E2$ and $M1$ interactions. These lowest-order, non-electric-dipole corrections to the dipole approximation lead to so-called *non-dipole* effects in the angular distributions of photoelectrons, described by [6]

$$\frac{d\sigma}{d\Omega} = \frac{\sigma}{4\pi}\left[1+\frac{\beta}{2}\left(3\cos^2\theta-1\right)+\left(\delta+\gamma\cos^2\theta\right)\sin\theta\cos\phi\right] \tag{2}$$

for 100% linearly polarized light. The non-dipole angular-distribution parameters γ and δ are attributable to interference terms between electric-dipole and electric-quadrupole interactions. Fig. 1 describes the geometry and the angles θ and ϕ.

Extensive measurements [7,8], focussing on noble-gas core levels (Ar K and Kr L) and photon energies above 2 keV, have begun to investigate non-dipole effects in photoelectron angular distributions in more detail.

In contrast, the present experiment concentrates on the N_2 $1s$ inner shell at relatively low photon energies ($\leq$1000 eV). Non-dipole effects are observed to be significant in this energy regime and measurable at energies close to threshold, in conflict with a common assumption

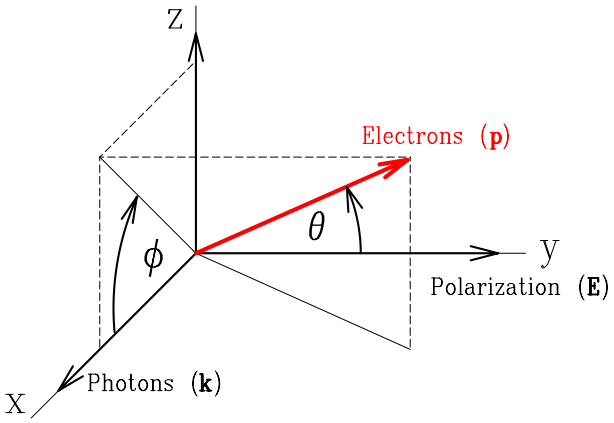

Figure 1: Geometry applicable to photoelectron angular-distribution measurements using polarized light. θ is the polar angle between the photon polarization vector ϵ and the momentum vector p of the photoelectron. ϕ is the azimuthal angle defined by the photon propagation vector k and the projection of p into the x-z plane.

in applications of photoelectron spectroscopy; namely, that the dipole approximation is valid for photon energies below 1 keV. The potential significance of these findings is nicely illustrated by comparison of the present results for the N_2 γ_{1s} parameter with a theory for atomic nitrogen [9], where the influence of non-dipole effects are expected to be much smaller.

EXPERIMENT

The experiments were performed on undulator beamline 8.0, [10], which covers the 100-1500 eV photon-energy range. The monochromator entrance slit was set to 70 μm and the exit slit to 100 μm yielding very high flux, because high photon resolution was not needed. During the measurements the ALS operated at 1.9 GeV in two-bunch mode with a photon pulse every 328 ns. Four time-of-flight (TOF) electron analyzers, equipped with microchannel plates for electron detection, collect spectra simultaneously at different angles. The total electron flight paths are 460 mm, and the analyzers have a full cone acceptance angle of 5°.
The interaction region is formed by an effusive gas jet intersecting the photon beam which has a diameter of about 2 mm. Energy resolution of the TOF analyzers with a focus size of 2 mm is 3% of the electron kinetic energy. Each spectrum was collected for about 600 s. We used either air or a mixture of air and xenon as our target gases. The abundance of Auger lines, especially for kinetic energies below 100 eV, provided for excellent calibration.

RESULTS

Figure 1 shows two superimposed spectra, both taken at the magic angle ($\theta = 54.7^o$), but at different ϕ angles. The spectra are scaled to the area of the N_2 KLL Auger lines. The obvious intensity differences between the N_2 $1s$ and satellite peaks in the two spectra are due entirely to non-dipole effects because both spectra are at the magic angle where the β parameter has no influence. For the dipole magic-angle analyzer the differential cross section in Eq. (2) reduces to the partial cross section; $E2$ and $M1$ effects vanish in the $\phi = 90°$ plane even if relativistic effects are included [11]. For the non-dipole analyzer,

$$\frac{d\sigma}{d\Omega} = \frac{\sigma}{4\pi}\left[1 + \sqrt{\frac{2}{27}}(3\delta + \gamma)\right], \qquad (3)$$

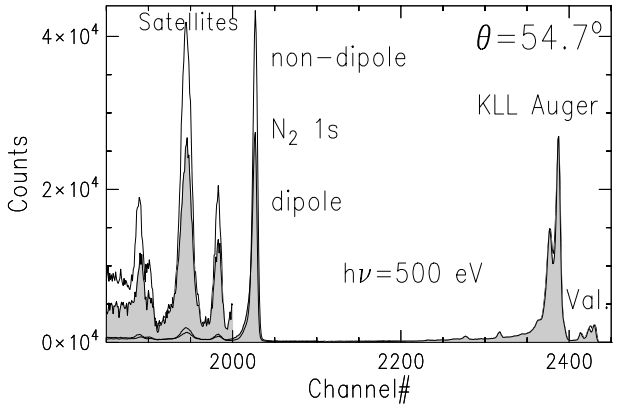

Figure 2: Photoelectron spectra of N_2 measured at a photon energy of 500 eV. The grey spectrum was taken with the dipole magic-angle analyzer and the other spectrum with the non-dipole analyzer. The spectra are normalized to the KLL Auger lines. The intensity differences in the N_2 1*s* and satellite lines between the two analyzers is due entirely to non-dipole effects.

which simplifies further for *s* subshells [6,12] in the non-relativistic approach where δ vanishes.

With our experimental geometry, it is possible to measure the γ parameter for *s* subshells directly if the degree of linear polarization is known by using the two magic angle analyzers. The data points in Fig. 3 show strong non-dipole contributions with a maximum of $\gamma = 1.3$ about 60 eV above the N_2 1*s* ionization threshold.

These non-dipole contributions originate from dipole integrals in the first-order correction to the dipole approximation. The observed deviations to the theoretical curve for atomic nitrogen are clearly due to molecular potential effects and according to theory [14] it is expected to appear only in molecules with degenerate states, such as N_2, O_2, CO_2 etc. but not CO, N_2O or similar molecules. The lack of correlation between the maximum and width of the absorption curve and the maximum and width of the data-point distribution suggests that it is not a shape-resonance effect. A theoretical interpretation is needed to fully explain the behavior of the γ-parameter. In the photon energy range between 600 eV and 1000 eV there is still a deviation between the theoretical curve for atomic nitrogen and the experimental data for molecular nitrogen. The molecular potential has a very strong

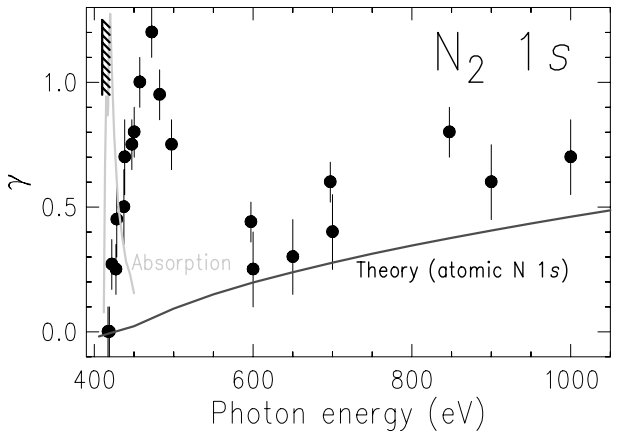

Figure 3: Electron angular anisotropy parameter γ for the N_2 1*s* photoline from threshold to $h\nu = 1000$ eV. The theoretical curve for atomic nitrogen is from Lajohn and Pratt [9] and the N_2 absorption curve from Kempgens et al. [13].

influence on the non-dipole electron angular distributions far above threshold unlike the shape-resonance that governs the β-parameter just above threshold before it assumes atomic like behavior.
The present results illustrate that any photoemission experiment, whether on gases, solids, or surfaces, can be so influenced at relatively low photon energies, pointing to a general need for caution in interpreting angle-resolved photoemission data.

ACKNOWLEDGMENTS

The authors thank the staff of the ALS for their support, the IBM, LBNL, LLNL, the University of Tennessee, and Tulane University collaboration for beam time at beamline 8.0, and R. H. Pratt for fruitful discussions. This research is funded by the National Science Foundation (NSF, PHY-9303915), the Department of Energy (DOE EPSCOR), Research Corporation, and The Petroleum Research Fund. The ALS is supported by the DOE under Contract No. DE-AC03-76SF00098. O.H. acknowledges financial support by the Deutsche Forschungsgemeinschaft. R.W. is grateful for a Feodor-Lynen-Fellowship.

REFERENCES

1. H.A. Bethe and E.E. Salpeter, *Quantum Mechanics of One- and Two-Electron Atoms* (Springer-Verlag, Berlin, 1957).
2. S.T. Manson and D. Dill, in *Electron Spectroscopy: Theory, Techniques, and Applications*, Vol. 2, ed. by C.R. Brundle and A.D. Baker (Academic, N.Y., 1978).
3. J. Cooper and R.N. Zare, J. Chem. Phys. **48**, 942 (1968).
4. M.O. Krause, Phys. Rev. **177**, 151 (1969).
5. For unpolarized incident light, $\beta/2$ is replaced by $-\beta/4$ in Eq. (1), and θ is measured between the propagation vectors of the photon and the photoelectron. Otherwise, the essential physics is the same.
6. J.W. Cooper, Phys. Rev. A **42**, 6942 (1990); **47**, 1841 (1993).
7. B. Krässig, M. Jung, D.S. Gemmell, E.P. Kanter, T. LeBrun, S.H. Southworth, and L. Young, Phys. Rev. Lett. **75**, 4736 (1995).
8. M. Jung, B. Krässig, D.S. Gemmell, E.P. Kanter, T. LeBrun, S.H. Southworth, and L. Young, Phys. Rev. A **54**, 2127 (1996).
9. L. Lajohn and R.H. Pratt (private communication).
10. R.C.C. Perera, Nucl. Instrum. Methods **A319**, 277 (1992).
11. J.H. Scofield, Phys. Rev. A **40**, 3054 (1989); Phys. Scripta **41**, 59 (1990).
12. M. Ya. Amusia and N.A. Cherepkov, *Case Studies in Atomic Physics*, Vol. 5 (North-Holland, Amsterdam, 1975), p. 47.
13. B. Kempgens, A. Kivimäki, M. Neeb, H.M. Köppe, A.M. Bradshaw, and J. Feldhaus, J. Phys. B **29**, 5389 (1996).
14. P. Langhoff (private communication).

Principal Investigator: Dennis W. Lindle, University of Nevada, Las Vegas. Email: lindle@nevada.edu. Telephone: 702-895-4426.